Crane Modeling and Simulation in Offshore Structure Building Industry

Namkug Ku, Sol Ha, and Myoung-Il Roh

***Abstract*—To increase the lifting capacity and minimize the cost and time for building a ship and offshore structure, block lifting with multi-cranes becomes more and more danger. In this paper, therefore, dynamic response analysis of the multi-cranes is performed for block lifting operation. By this simulation, one can confirm the dynamic effects, such as dynamic motion and load, to prevent fatal accidents during the multi-crane operation. The crane system consists of several bodies. These bodies are connected with various types of joints and wire rope. To carry out the dynamic simulation, therefore, the crane system is modeled as a multi-body system. There are several types of crane, such as a goliath crane, jib crane, and floating crane, etc. Among them, the floating crane is operated on the sea water. Therefore the hydrostatic force and linearized hydrodynamic force are considered as the external forces acting on the floating crane. Using the dynamics simulation program developed in this paper, a dynamic response simulation of several cases of block lifting with multi-cranes are carried out, and the simulation results are validated by comparing them with the measured data from the shipyard. Moreover, the simulation results can be applied to the structural analysis for evaluate the dynamic effects on the block.**

***Index Terms*—Dynamic simulation, modeling and simulation, multi-body system, large scale manufacturing, structural analysis.**

I. Introduction

Recently, the shipyard has been manufacturing the offshore structure blocks as large as possible for minimize the building cost and time. But weight of these blocks often exceeds the lifting capability of the crane. Thus to solve this problem, the shipyard has started to use multiple cranes to lift the heavy loads.

Fig. 1 shows various situations using the multi-crane. Fig. 1 (a) shows operation of block turnover using 2 goliath cranes, which is one of the most important equipment in shipyard, Fig. 1 (b) shows launching a ship, which is built outside dock, to the ocean using 2 floating cranes which can generally transport the blocks heavier than the ones carried by goliath crane, and Fig. 1 (c) shows transportation of the blocks to the dock using 2 Jib cranes. These transporting operations are more dangerous than using single crane, thus it is important to have simulations to insure the safety of the operation in advance.

The crane systems in Fig. 1 are all multi-body system which the multiple rigid bodies are jointed together, therefore the shipyard recently want to use the general analysis program for its dynamic response analysis. But the disadvantage of using the general analysis program for dynamic response of multi-body system is that it is difficult to consider its exact fluid dynamic, in specific, it's hard to analyze its hydrostatic and hydrodynamic force.

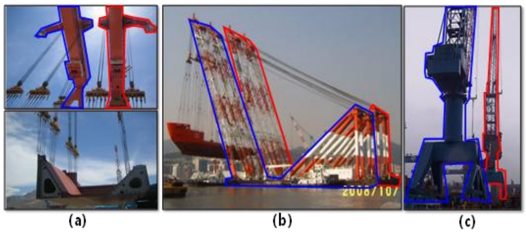

Fig. 1. Various cases of heavy load transportation using multi-crane in the offshore structure building industry: (a) two goliath cranes; (b) two floating cranes; and (c) two jib cranes.

In a case of floating cranes for example, the crane is constantly experiencing hydrodynamic forces during the lifting operation. Therefore in this paper, the kernels are developed that can analyze the dynamic response of the multi-body system and calculate the hydrostatic, hydrodynamic, and wind forces.

In this paper, the research about the commercial kernel of dynamic analysis for multi-body system is discussed first. Then, the kernel of dynamic analysis developed in this research is discussed, and the developed kernel for determining external forces is discussed. After that, the result of simulation for dynamic response analysis of multi-crane using the developed program will be discussed, and lastly the conclusion and further plan for the research will be considered.

II. Related Work

ADAMS (Automatic Dynamic Analysis of Mechanical Systems) is a software system that consists of a number of integrated programs that aid an engineer in performing three-dimensional kinematic and dynamic analysis of mechanical systems [1], [2] ADAMS generates equations of motion for multi-body systems using augmented formulation. The user can define any multi-body system composed of several rigid and flexible bodies that are interconnected by joints. ADAMS supplies various types of joints, such as fixed, revolute, and spherical joints. Various external forces can also be applied to the multi-body systems, but the hydrostatic and hydrodynamic forces, which are the dominant forces exerted on the floating platform, cannot be handled by ADAMS.

ODE (Open Dynamics Engine) is an open-source library

Manuscript received October 20, 2013; revised January 7, 2014.

The authors are with the Education and Research Center for Creative Offshore Plant Engineers, Engineering Research Institute, and Department of naval architecture and ocean engineering in Seoul National University, South Korea (e-mail: knk80@snu.ac.kr).

DOI: 10.7763/IJCTE.2014.V6.875

for simulating multi-body dynamics [3]. Similar to ADAMS, ODE derives equations of motion for multi-body systems using augmented formulation. ODE can treat only rigid bodies, however, not flexible bodies. Moreover, ODE cannot handle hydrostatic and hydrodynamic forces.

RecurDyn [4] is a three-dimensional simulation software that combines dynamic response analysis and finite element analysis tools for multi-body systems. It is 2 to 20 times faster than other dynamic solutions because of its advanced fully recursive formulation. Various joints and external forces can also be applied to the multi-body systems, but RecurDyn cannot handle hydrostatic and hydrodynamic forces.

This study presents the development of a dynamics kernel for the dynamic analysis of offshore structures such as semi-submersible drilling rig or drill ship. The equations of motion for multi-body systems were derived using recursive formulation. Moreover, the external force calculation module can generate hydrostatic force by considering the nonlinear effects and the linearized hydrodynamic force as external forces.

It is possible to interface these general programs with hydrodynamics using user-subroutine. For example, Jonkman developed a module called “HydroDyn” for calculating hydrodynamic force in time domain and interface it with other program [5]. For calculating hydrodynamic force in time domain, Jonkman transforms the analysis results from “WAMIT”, which is a commercial program for calculating hydrodynamic force in frequency domain, into time domain using Cummins equation. In other words, the analysis results from “WAMT” are required to use “Hydrodyn”. In this research, to make the developed kernel independent from any other programs, 3D Rankine panel method is applied for direct calculation of hydrodynamic force in time domain. To interface 3D Rankine panel method with the existing programs of dynamic response analysis for multi-body, input of hydrodynamic force is not enough. To increase numerical stability, it is required to modify the mass and inertia of the floating body using added mass. Therefore it is not easy to interface with other commercial programs. Moreover, as mentioned above, to make the developed kernel independent from any other programs, the functions for analyzing dynamic response of multi-body and calculating hydrostatic and dynamic force are integrated together. Table I shows the features of the different dynamics kernels that were compared in this study.

TABLE I: COMPARISON OF THE FEATURES OF THE DEVELOPED DYNAMICS KERNEL IN THIS STUDY WITH COMMERCIAL DYNAMICS KERNEL

	This study	ADAMS	ODE	RecurDyn
Multi-body formulation	Recursive formulation	Augmented formulation	Augmented formulation	Recursive formulation
Various joints	O	O	O	O
Flexible body	X	O	X	O
Hydrostatic force	O	Δ	Δ	Δ
Linearized hydrodynamic force	O	Δ	Δ	Δ

*(O: Supported; Δ: Can be only interfaced by the developer of the dynamics kernel)

III. DEVELOPMENT OF KERNEL OF DYNAMIC ANALYSIS FOR MULTI-BODY SYSTEM

The kernel of dynamic analysis is developed for the multi-body system. In this section, the recursive formulation applied for the construction of kinematic equation of multi-body system is explained.

A. Forward and Inverse Dynamics

The dynamics of a rigid-body system are described by its equation of motion, which specifies the relationship between the forces that act on the system and the accelerations they produce. The main concern in this section is the algorithms for the following two particular calculations.

- Forward dynamics: The calculation of the acceleration response of a given rigid-body system to a given applied force
- Inverse dynamics: The calculation of the force that must be applied to a given rigid-body system to produce a given acceleration response

Forward dynamics is used mainly in simulation. Inverse dynamics will be explained first, however, since it is easier than forward dynamics in the manner of the explanation of the recursive formulation [6].

B. Inverse Dynamics of Recursive Formulation

The equations of motion for each body of the multi-body system based on recursive formulation can be summarized as following.

$$\hat{\mathbf{v}}_i = {}^i\mathbf{X}_{i-1} \cdot \hat{\mathbf{v}}_{i-1} + \mathbf{S}_i \cdot \dot{q}_i \tag{1}$$

$$\hat{\mathbf{a}}_i = {}^i\mathbf{X}_{i-1} \cdot \hat{\mathbf{a}}_{i-1} + \mathbf{S}_i \cdot \ddot{q}_i + \dot{\mathbf{S}}_i \cdot \dot{q}_i + \hat{\mathbf{v}}_i \times \mathbf{S}_i \cdot \dot{q}_i \tag{2}$$

$$\hat{\mathbf{f}}_i^B = \hat{\mathbf{I}}_i \cdot \hat{\mathbf{a}}_i + \hat{\mathbf{v}}_i \times^* \hat{\mathbf{I}}_i \cdot \hat{\mathbf{v}}_i \tag{3}$$

$$\hat{\mathbf{f}}_i = \hat{\mathbf{f}}_i^B + {}^i\mathbf{X}_{i+1}^* \cdot \hat{\mathbf{f}}_{i+1} - \hat{\mathbf{f}}_i^{ext} \tag{4}$$

$$\tau_i = \mathbf{S}_i^T \cdot \hat{\mathbf{f}}_i \text{ -} \tag{5}$$

In here, $\hat{\mathbf{v}}_i$ is velocity vector(6 elements) of body ©, $\hat{\mathbf{a}}_i$ is acceleration vector(6 elements) of body ©, q_i is generalized coordinate(joint value), $\mathbf{S}_i$ is velocity transformation matrix, $\mathbf{I}_i$ is mass and mass moment of inertia of body ©, $\hat{\mathbf{f}}_i^B$ is resultant force exerted on body ©, $\hat{\mathbf{f}}_i^{ext}$ is external force exerted on body ©, $\hat{\mathbf{f}}_i$ is force across the joint ©, and τ_i is force generated by joint © (generalized force). In inverse dynamics, since the positions q_i, velocities $\dot{q}_i$, and accelerations $\ddot{q}_i$ of generalized coordinates are given, the velocities $\hat{\mathbf{v}}_i$ and accelerations $\hat{\mathbf{a}}_i$ of each body can be computed. Furthermore, the forces $\hat{\mathbf{f}}_i$ and the generalized forces τ_i, which should be exerted on each link, can be also computed in a recursive fashion [6], [7].

For example, the equations of motion for the three-link multi-body system can be formulated as shown in Fig. 2.

Equations of motion for link 1

$\hat{\mathbf{v}}_1 = {}^1\mathbf{X}_0 \boxed{\cdot \hat{\mathbf{v}}_0} + \mathbf{S}_1 \cdot \dot{q}_1$ ·· (1-a)

$\hat{\mathbf{a}}_1 = {}^1\mathbf{X}_0 \boxed{\cdot \hat{\mathbf{a}}_0} + \mathbf{S}_1 \cdot \ddot{q}_1 + \dot{\mathbf{S}}_1 \cdot \dot{q}_1 + \hat{\mathbf{v}}_1 \times \mathbf{S}_1 \cdot \dot{q}_1$ ·· (1-b)

$\hat{\mathbf{f}}_1^B = \hat{\mathbf{I}}_1 \cdot \hat{\mathbf{a}}_1 + \hat{\mathbf{v}}_1 \times^* \hat{\mathbf{I}}_1 \cdot \hat{\mathbf{v}}_1$ ·· (1-c)

$\hat{\mathbf{f}}_1 = \hat{\mathbf{f}}_1^B + {}^1\mathbf{X}_2^* \cdot \hat{\mathbf{f}}_2 - \hat{\mathbf{f}}_1^{ext}$ ·· (1-d)

$\tau_1 = \mathbf{S}_1^{\,T} \cdot \hat{\mathbf{f}}_1$ ·· (1-e)

Equations of motion for link 2

$\hat{\mathbf{v}}_2 = {}^i\mathbf{X}_1 \cdot \hat{\mathbf{v}}_1 + \mathbf{S}_2 \cdot \dot{q}_2$ ·· (2-a)

$\hat{\mathbf{a}}_2 = {}^2\mathbf{X}_1 \cdot \hat{\mathbf{a}}_1 + \mathbf{S}_2 \cdot \ddot{q}_2 + \dot{\mathbf{S}}_2 \cdot \dot{q}_2 + \hat{\mathbf{v}}_2 \times \mathbf{S}_2 \cdot \dot{q}_2$ ·· (2-b)

$\hat{\mathbf{f}}_2^B = \hat{\mathbf{I}}_2 \cdot \hat{\mathbf{a}}_2 + \hat{\mathbf{v}}_2 \times^* \hat{\mathbf{I}}_2 \cdot \hat{\mathbf{v}}_2$ ·· (2-c)

$\hat{\mathbf{f}}_2 = \hat{\mathbf{f}}_2^B + {}^2\mathbf{X}_3^* \cdot \hat{\mathbf{f}}_3 - \hat{\mathbf{f}}_2^{ext}$ ·· (2-d)

$\tau_2 = \mathbf{S}_2^{\,T} \cdot \hat{\mathbf{f}}_2$ ·· (2-e)

Equations of motion for link 3

$\hat{\mathbf{v}}_3 = {}^3\mathbf{X}_2 \cdot \hat{\mathbf{v}}_2 + \mathbf{S}_3 \cdot \dot{q}_3$ ·· (3-a)

$\hat{\mathbf{a}}_3 = {}^3\mathbf{X}_2 \cdot \hat{\mathbf{a}}_2 + \mathbf{S}_3 \cdot \ddot{q}_3 + \dot{\mathbf{S}}_3 \cdot \dot{q}_3 + \hat{\mathbf{v}}_3 \times \mathbf{S}_3 \cdot \dot{q}_3$ ·· (3-b)

$\hat{\mathbf{f}}_3^B = \hat{\mathbf{I}}_3 \cdot \hat{\mathbf{a}}_3 + \hat{\mathbf{v}}_3 \times^* \hat{\mathbf{I}}_3 \cdot \hat{\mathbf{v}}_3$ ·· (3-c)

$\hat{\mathbf{f}}_3 = \hat{\mathbf{f}}_3^B + {}^3\mathbf{X}_4^* \boxed{\cdot \hat{\mathbf{f}}_4} - \hat{\mathbf{f}}_3^{ext}$ ·· (3-d)

$\tau_3 = \mathbf{S}_3^{\,T} \cdot \hat{\mathbf{f}}_3$ ·· (3-e)

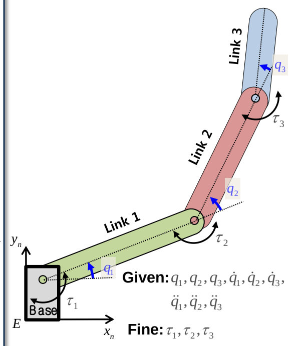

Fig. 2. Example of an inverse dynamics problem: three-link multi-body system.

1) The velocity of link 1, $\hat{\mathbf{v}}_1$, can be determined using (1-a), since the velocity of the base, $\hat{\mathbf{v}}_0$, is zero. Then the velocities of the other bodies can be determined using (2-a) and (3-a).
2) The acceleration of link 1, $\hat{\mathbf{a}}_1$, can be determined using (1-b), since the acceleration of the base, $\hat{\mathbf{a}}_0$, is zero. Then the accelerations of the other bodies can be determined using (2-b) and (3-b).
3) Because the velocities and acceleration are determined, the resultant forces can be determined using (1-c), (2-c), and (3-c).
4) Because link 4 does not exist, the force, $\hat{\mathbf{f}}_4$, exerted on link 4 by link 3 is zero. Therefore, the force, $\hat{\mathbf{f}}_3$, exerted on link 3 by link 2 can be determined using (3-d). Then forces $\hat{\mathbf{f}}_2$ and $\hat{\mathbf{f}}_1$ can be determined using (2-d) and (1-d).
5) Finally, the generalized forces τ_1, τ_2, and τ_3 can be determined by suppressing the constraint forces from forces $\hat{\mathbf{f}}_1$, $\hat{\mathbf{f}}_2$, and $\hat{\mathbf{f}}_3$.

C. Forward Dynamics of Recursive Formulation

For the simple explanation of inverse dynamics, (1) ~ (5) will be expressed in a more compact form through the following steps.

1) Because $\dot{q}_i$ is given and velocities $\hat{\mathbf{v}}_i$ can be determined in the recursive fashion using only (1), $\hat{\mathbf{v}}_i$ will be considered as given.
2) When the velocities $\hat{\mathbf{v}}_i$ are considered a given, the last term of (2), $\dot{\mathbf{S}}_i \cdot \dot{q}_i + \hat{\mathbf{v}}_i \times \mathbf{S}_i \cdot \dot{q}_i$, can be determined without considering the other equations. Therefore, it will be denoted as $\mathbf{c}_i$ and considered a given value.

$$\mathbf{c}_i = \dot{\mathbf{S}}_i \cdot \dot{q}_i + \hat{\mathbf{v}}_i \times \mathbf{S}_i \cdot \dot{q}_i \tag{6}$$

3) As shown in (7), when the new notation $\hat{\mathbf{f}}_i^{B'}$ denotes $\hat{\mathbf{f}}_i^{B} - \hat{\mathbf{f}}_i^{ext}$, (3) and (4) are rewritten as (8) and (9).

$$\hat{\mathbf{f}}_i^{B'} = \hat{\mathbf{f}}_i^{B} - \hat{\mathbf{f}}_i^{ext} \tag{7}$$

$$\hat{\mathbf{f}}_i^{B'} = \hat{\mathbf{I}}_i \cdot \hat{\mathbf{a}}_i + \hat{\mathbf{v}}_i \times^* \hat{\mathbf{I}}_i \cdot \hat{\mathbf{v}}_i - \hat{\mathbf{f}}_i^{ext} \tag{8}$$

$$\hat{\mathbf{f}}_i = \hat{\mathbf{f}}_i^{B'} + {}^i\mathbf{X}_{i+1}^* \cdot \hat{\mathbf{f}}_{i+1} \tag{9}$$

4) Because $\hat{\mathbf{f}}_i^{ext}$ is given, $\hat{\mathbf{v}}_i \times^* \hat{\mathbf{I}}_i \cdot \hat{\mathbf{v}}_i - \hat{\mathbf{f}}_i^{ext}$ can also be determined without considering the other equations. Therefore, it will be denoted as $\mathbf{p}_i$ and considered a given value.

$$\mathbf{p}_i = \hat{\mathbf{v}}_i \times^* \hat{\mathbf{I}}_i \cdot \hat{\mathbf{v}}_i - \hat{\mathbf{f}}_i^{ext} \ldots\ldots\ldots\ldots \tag{10}$$

By substituting (6), (8) ~ (10) into (2) ~ (5), (11) ~ (14) are derived.

$$\hat{\mathbf{a}}_i = {}^i\mathbf{X}_{i-1} \cdot \hat{\mathbf{a}}_{i-1} + \mathbf{S}_i \cdot \ddot{q}_i + \mathbf{c}_i \tag{11}$$

$$\hat{\mathbf{f}}_i^{B'} = \hat{\mathbf{I}}_i \cdot \hat{\mathbf{a}}_i + \mathbf{p}_i \tag{12}$$

$$\hat{\mathbf{f}}_i = \hat{\mathbf{f}}_i^{B'} + {}^i\mathbf{X}_{i+1}^* \cdot \hat{\mathbf{f}}_{i+1} \tag{13}$$

$$\tau_i = \mathbf{S}_i^{\,T} \cdot \hat{\mathbf{f}}_i \tag{14}$$

(11) ~ (14) can be rearranged into (15) ~ (18), and they are the equations of motion for the forward dynamics of the multi-body system based on recursive formulation.

$$\hat{\mathbf{a}}_i = {}^i\mathbf{X}_{i-1} \cdot \hat{\mathbf{a}}_{i-1} + \mathbf{S}_i \cdot \ddot{q}_i + \mathbf{c}_i \tag{15}$$

$$\ddot{q}_i = \left(\mathbf{S}_i^T \hat{\mathbf{I}}_i^A \mathbf{S}_i\right)^{-1} \left(\tau_i - \mathbf{S}_i^T \left(\hat{\mathbf{I}}_i^A \left({}^i\mathbf{X}_{i-1} \hat{\mathbf{a}}_{i-1} + \mathbf{c}_i\right) + \mathbf{p}_i^A\right)\right) \tag{16}$$

$$\hat{\mathbf{I}}_i^A = \hat{\mathbf{I}}_i + {}^i\mathbf{X}_{i+1}^* \cdot \hat{\mathbf{I}}_{i+1}^A \cdot {}^{i+1}\mathbf{X}_i - {}^i\mathbf{X}_{i+1}^* \cdot \hat{\mathbf{I}}_{i+1}^A \cdot \mathbf{S}_{i+1} \cdot \left(\mathbf{S}_{i+1}^T \hat{\mathbf{I}}_{i+1}^A \mathbf{S}_{i+1}\right)^{-1} \mathbf{S}_{i+1}^T \hat{\mathbf{I}}_{i+1}^A \, {}^{i+1}\mathbf{X}_i \tag{17}$$

$$\begin{aligned} \mathbf{p}_i^A = {} & \mathbf{p}_i + {}^i\mathbf{X}_{i+1}^* \cdot \mathbf{p}_{i+1}^A + {}^i\mathbf{X}_{i+1}^* \cdot \hat{\mathbf{I}}_{i+1}^A \cdot \mathbf{c}_{i+1} + \\ & {}^i\mathbf{X}_{i+1}^* \cdot \hat{\mathbf{I}}_{i+1}^A \cdot \mathbf{S}_{i+1} \cdot \left(\mathbf{S}_{i+1}^T \hat{\mathbf{I}}_{i+1}^A \mathbf{S}_{i+1}\right)^{-1} \left(\tau_{i+1} - \mathbf{S}_{i+1}^T \left(\hat{\mathbf{I}}_{i+1}^A \mathbf{c}_{i+1} + \mathbf{p}_{i+1}^A\right)\right) \end{aligned} \tag{18}$$

Based on the equations of motion for the forward and inverse dynamics, the kernel of dynamic analysis for multi-body system is developed.

IV. Verification of the Developed Kernel

In this section, the developed kernel is verified before the dynamic response analysis of the multi-body system is performed by comparing it with other commercial kernels for two test models.

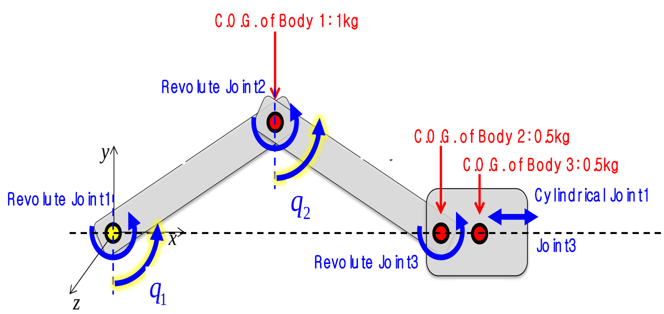

Fig. 3. Multi-body system composed of three bodies, three revolute joints, one cylindrical joint and one closed loop.

The first test model is a multi-body system composed of three bodies, three revolute joints, one cylindrical joint, and one closed loop, as shown in Fig. 3.

Body 1 is attached to the base by revolute joint 1, and body 2 is connected to body 1 by revolute joint 2. Body 3 is attached to body 2 with revolute joint 3, and moves perpendicular to the x axis due to cylindrical joint 1.

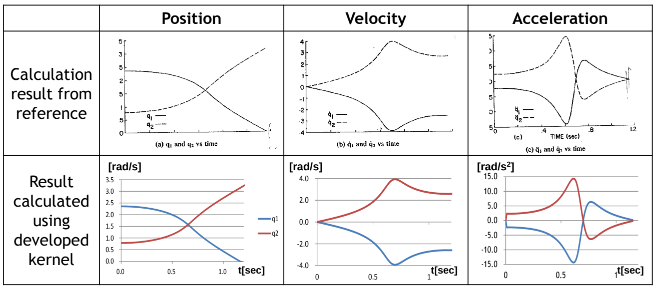

Fig. 4. Results of the simulation of the position, velocity, and acceleration of generalized coordinates q1 and q2 compared with those yielded by the reference.

The position, velocity, and acceleration of the generalized coordinates q_1 and q_2 illustrated in Fig. 3 were compared with those yielded by the reference [8]. The results match well, as shown in Fig. 4

As shown in Fig. 5, the third test model is a multi-body system composed of eight bodies and 10 revolute joints. Also, the system has three closed loops. This model is used to verify the dynamic codes developed in the 1980s.

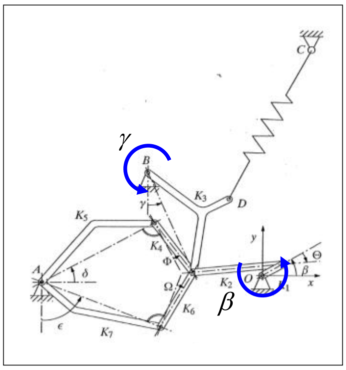

Fig. 5. Generalized coordinates β, and γ of the multi-body system.

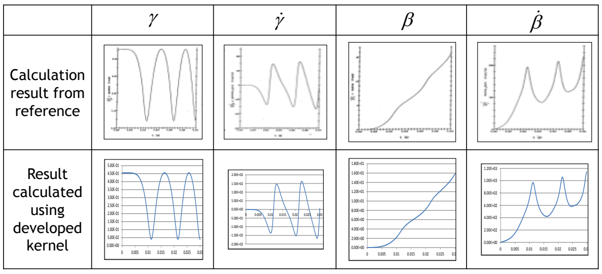

Fig. 6. Simulation results of the position and velocity of the generalized coordinates β, and γ compared with those yielded by reference.

The position, velocity, and acceleration of generalized coordinates β and γ illustrated in Fig. 6 were compared with those yielded by the reference [2]. The results match perfectly.

V. External Force for Dynamic Response Analysis

The recursive formulation used to construct the equation of motion can be used for dynamic response analysis after the input of external force. The external forces considered in this simulation are hydrostatic force with non-linear effect, linearized hydrodynamic force, gravitational force, and wind force.

A. Hydrostatic Force

The hydrostatic force applied to floating platform is calculated while considering its instantaneous position and is expressed as seen in (19) [9].

$$\mathbf{f}^{e}_{Hydrostatic} = \rho_{SW} g[0\,;0\,;\int_V dV\,;\int_V y_{Buoyancy} dV\,;-\int_V x_{Buoyancy} dV\,;0\,]^T \tag{19}$$

In here, ρ_{SW} is density of the sea water, g is gravitational acceleration, V is submerged volume of the floating body, and $x_{Buoyancy}$, $y_{Buoyancy}$ are represent the coordinates of center of buoyancy, respectively.

B. Hydrodynamic Force

The hydrodynamic force is calculated in time domain using 3D Rankine panel method. The governing equation is Laplace equation (20).

$$\nabla^2\phi = 0, \quad \phi = \phi_I + \phi_d \tag{20}$$

where ϕ_I is incident wave potential, and ϕ_d is disturbed potential.

The incident wave potential needs to satisfy the boundary condition seen below. (21) ~ (24) are linearized kinematic free surface, linearized dynamic free surface, bottom and radiation boundary conditions, respectively.

$$\frac{\partial\phi_I}{\partial z} - \frac{\partial\eta_I}{\partial t} = 0 \quad at \quad z = 0 \tag{21}$$

$$\frac{\partial\phi_I}{\partial t} + g\eta_I = 0 \quad at \quad z = 0 \tag{22}$$

$$\left.\frac{\partial\phi_I}{\partial z}\right|_{z=-h} = 0 \tag{23}$$

$$\begin{gathered}\phi_I(x,y,z,t) = \phi_I(x,y,z,t+T)\\ \phi_I(x,y,z,t) = \phi_I(x+L,y,z,t)\\ \phi_I(x,y,z,t) = \phi_I(x,y+L,z,t)\end{gathered} \tag{24}$$

where η_I, T, L is the elevation, period and length of incident wave.

The disturbed wave potential needs to satisfy the boundary condition seen below. (25) is body boundary condition, (26) is kinematic free surface boundary condition including artificial damping, and (27) is dynamic free surface boundary condition.

$$\frac{\partial\phi_d}{\partial \mathbf{n}} = \frac{\partial\boldsymbol{\delta}}{\partial t}\mathbf{n} - \frac{\partial\phi_I}{\partial \mathbf{n}}, \boldsymbol{\delta} = \boldsymbol{\xi}_T + \boldsymbol{\xi}_R \times \mathbf{r} \tag{25}$$

$$\frac{\partial\eta_d}{\partial t} = \frac{\partial\phi_d}{\partial z} - 2\nu\eta_d + \frac{\nu^2}{g}\phi_d \tag{26}$$

$$\frac{\partial \phi_d}{\partial t} + g\eta_d(t+dt) = 0 \tag{27}$$

where δ is position vector of the panel of floating body defined in inertial coordinate system, r is position vector of the panel of floating body defined in body-fixed coordinate system, ξ_T is position vector $(q_{P,1}, q_{P,2}, q_{P,3})$ of center of mass for object defined in inertia coordination, ξ_R is angular vector $(q_{P,4}, q_{P,5}, q_{P,6})$ defining the orientation of body-fixed coordinate system, η_d is wave elevation of the disturbed potential, and ν represents radiation coefficient.

Problems defined as above can be solved as follows. Incident wave potential ϕ_I have analytic solution (28).

$$\phi_I = \frac{g}{\omega} A e^{kz} \sin\left(kx\cos\theta + ky\sin\theta - \omega t\right) \tag{28}$$

where A is wave amplitude, k is wave number, θ is wave direction, ω is wave frequency.

Then disturbed potential ϕ_d is calculated using numerical method. In this case, the Green's second identity is used as seen in (29), and for G the 3D Rankine Source in (30) is used [10].

$$\phi_d = \iint_{S_{Body}} \left(\phi_d \frac{\partial G}{\partial n} - G\frac{\partial \phi_d}{\partial n}\right) dS + \iint_{S_F} \left(\phi_d \frac{\partial G}{\partial n} - G\frac{\partial \phi_d}{\partial n}\right) dS \tag{29}$$

$$G(\mathbf{x}, \mathbf{x}') = \frac{1}{4\pi}\frac{1}{|\mathbf{x} - \mathbf{x}'|} \tag{30}$$

In here, x is position vector of 3D Rankine source, x' is position vector of panels, S_{body} is body surface, and S_F is free surface.

To increase the numerical stability of this procedure, when we calculate acceleration of the ship at time ($t+dt$), $\mathbf{a}(t+dt)$, $\mathbf{m}_{add} \times \mathbf{a}(t)$ is considered as the additional external force with the hydrodynamic force at time (t+1), and $\mathbf{m}_{add}$ is added to real mass of the floating body. This is the reason why it is not very simple to apply the 3D Rankine panel method to the commercial program for multi-body response analysis. In here, $\mathbf{m}_{add}$ is added mass and it is also calculated using 3D Rankine panel method.

VI. Simulation of Launching a Ship Using Two Floating Crane

Fig. 1 (b) shows a case of using 2 floating cranes for launching a ship built on land due to the shortage of dock. The weight of the constructed ship in this case is 3,800ton before setting up the accommodations and other equipment. The capacity of the floating crane used in this process is 3,000ton each. The reason for using two floating cranes is due to the weight of ship exceeding the capability of single floating crane. For this simulation, the incident wave, whose amplitude, frequency, and direction are 0.5m, 0.628 rad/sec, 45 degree, respectively, are applied.

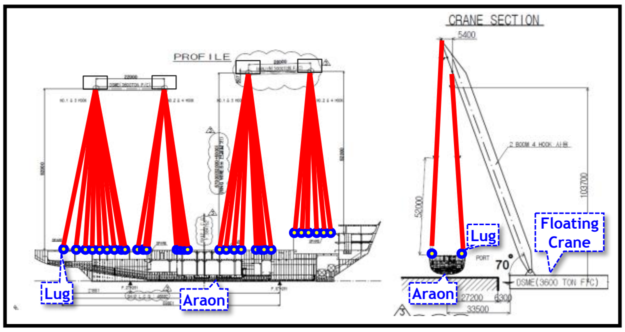

Fig. 7. The lug arrangement for lunching process of the ship using two floating cranes.

Fig. 7 is the plan for connecting the floating crane and ship with wire rope.

The launching simulation is processed in order as seen below, and its result is shown in Fig. 8.

1) Ship is placed on land.
2) hoisting-up the ship
3) The floating crane is moved to side while carrying the ship.
4) hoisting-down the ship
5) The ship lunching complete and the ship is floating.

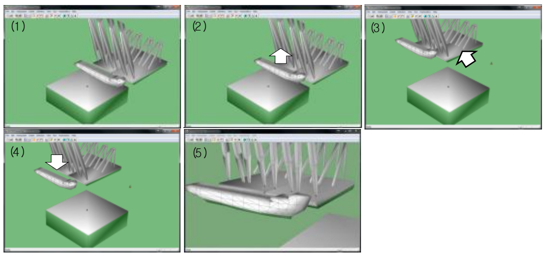

Fig. 8. The result of the simulation for the lunching process of the ship using two floating crane.

Fig. 9 shows the result of simulation that is the tension of two wire ropes numbered H3, H4 among total of 8 wire ropes. The tension changes according to the stage of the launching procedure, and we could confirm that the dynamic loads are 10 ~ 15% larger than the static loads.

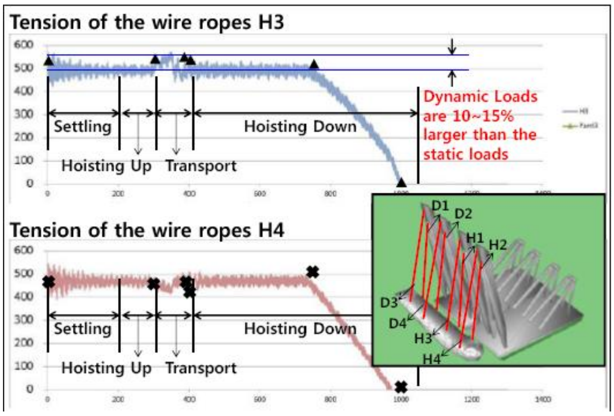

Fig. 9. Tension of the wire rope calculated from the simulation for the lunching process of the ship.

To validate the simulation results, it is compared with the measured data from the shipyard, which is marked with "triangle" in upper graph and "x" in lower graph. From the comparison, it is confirmed that the difference between simulation and measured data does not exceed 10%.

This 10% difference is mainly caused by uncertainty of synchronization between the cranes, and we are planning to consider this uncertainty as a factor of multi-crane simulation.

VII. Simulation for Block Turnover Using Two Goliath Cranes

Fig. 1 (a) shows the block lifting using 2 Goliath cranes. The weight of the block is 830ton which exceeds the capability of Goliath crane 600ton. Therefore, to move and turnover the block into the dock, two Goliath cranes is being used, and this process is being simulated.

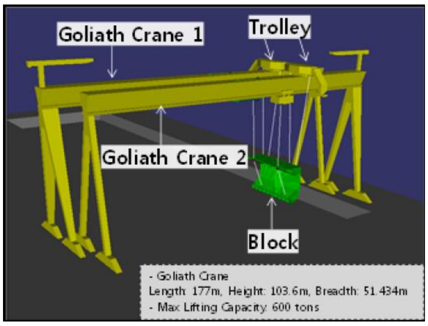

Fig. 10. The goliath cranes model for the simulation of the block turn-over process.

As seen in Fig. 10, the Goliath crane is composed of main body and trolley, and they are connected with prismatic joints. Based on this information, equations of motion are constructed using the kernel of dynamic analysis. The simulation is processed in order as seen below.

1) Hoisting-up the block

2) Goliath crane is moved in the direction of the dock and transports the block

3) turn-over the block

4) hoisting-down the block

In here, the process 1) and 2) are pictured in Fig. 11-(1), and process 3) is in Fig. 11-(2).

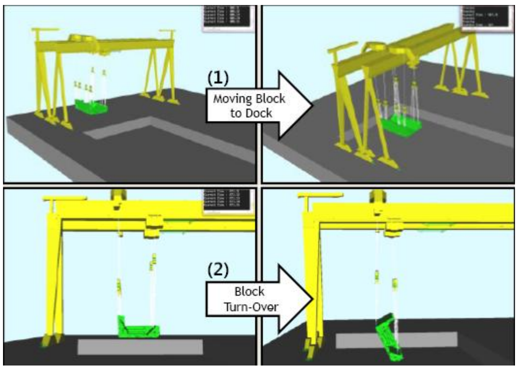

Fig. 11. the process of the block turn-over simulation.

Fig. 11 shows the result of simulation that is the tension of one wire rope in time among total of 6 wire ropes.

Since the weight of the block is 860ton and total of 6 wire ropes are used, the result of calculated tension of one wire being 140ton is reasonable. In addition, the dynamic change of tension can be predicted through this simulation before the manufacturing process in shipyard.

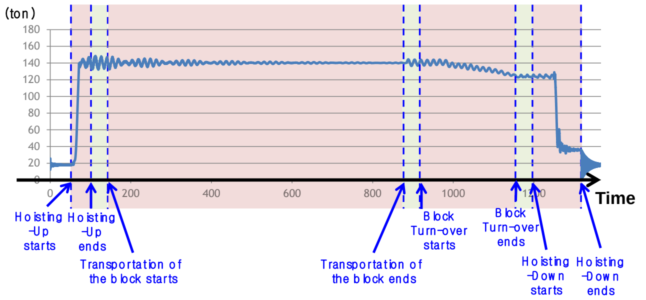

Fig. 12. Tension of the wire rope calculated from the simulation for the block turn-over process.

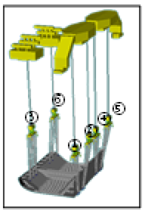

Line Num.	Max. Static Load	Max. Dynamic Load
①	140ton	166ton
②	112ton	134ton
③	195ton	210ton
④	151ton	171ton
⑤	124ton	150ton
⑥	212ton	224ton

Fig. 13. Maximum static and dynamic tension of the wire rope calculated from the simulation.

Fig. 13 shows the maximum static and dynamic tension of the wire rope calculated from the simulation. Using this simulation results, we can evaluate that how much the dynamic behavior of this manufacturing process effects on the block in structural aspects. Fig. 14 shows the results of structural analysis using the maximum loads. From this structural analysis, we can evaluate the maximum stress and deformation increase by 22.75% and 12.28% respectively, when the dynamic effects are considered.

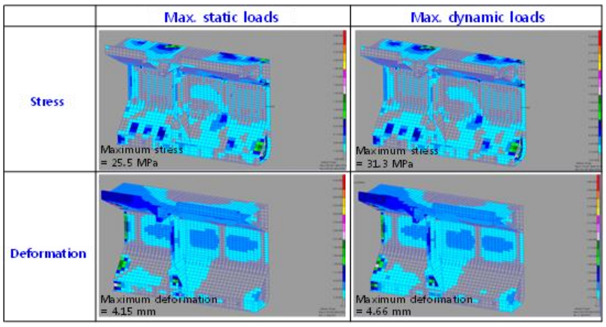

Fig. 14. the results of structural analysis using the maximum static and dynamic loads.

VIII. Conclusion and Further Research Plan

In this research, the kernel of dynamic analysis for multi-body system is developed. To calculate the suitable external forces for the various types of the cranes, the modules for determining hydrostatic, hydrodynamic, and wind forces are developed. The developed kernel and modules are verified by comparison with commercial software.

The modules are integrated with the kernel of dynamic analysis. Using the developed program, the dynamic response analysis for transportation of heavy load by multi-crane is performed. The results of the simulation are compared with the data measured from the shipyards. As a result of the comparison, we conclude the modules are well implemented for dynamic analysis of block lifting using multi-cranes. Moreover, the simulation results can be applied to the structural analysis for evaluate the dynamic effects on the block.

In further research, this simulation program will be applied to other various simulations in order to enhance its liability. Moreover, other several functions, for example, the equalizer, the module for calculating contact force between the wire rope and body, etc., will be developed to make this program can consider more field environment.

ACKNOWLEDGMENT

This study was partially supported by the Industrial Strategic Technology Development Program (10035331, Simulation-based Manufacturing Technology for Ships and Offshore Plants) funded by the Ministry of Knowledge Economy (MKE) of the Republic of Korea and by the Brain Korea 21 plus program of the Marine Technology Education and Research Center, the Research Institute of Marine Systems Engineering, and the Engineering Research Institute of Seoul National University.

REFERENCES

[1] N. Orlandea, M. A. Chace, and D. A. Calahan, “A sparsity-oriented approach to the dynamic analysis and design of mechanical systems-part 1 and 2,” *Journal of Engineering for Industry, Transactions of the ASME*, vol. 99, no. 3, pp. 773-779, 1977.
[2] W. Schiehlen, *Multibody Systems Handbook*, Springer, pp. 361-402, 1990.
[3] R. Smith, *Open dynamics Engine v0.5 User Guide*, pp. 15-20, 2006.
[4] FunctionBay, Inc., *RecurDyn V7R5 Release Notes*, 2011.
[5] J. M. Jonkman, “Dynamics of offshore floating wind turbines - model development and verification,” *Wind Energy*, 2009.
[6] R. Featherstone, *Rigid body Dynamics*, Springer, 2008.
[7] J. Y. S. Luh, “On-line computational scheme for mechanical manipulators,” *Journal of Dynamic Systems, Measurement, and Control*, vol. 102, pp. 69-76, 1980.
[8] E. J. Haug, *Intermediate Dynamics*, Prentice-hall, 1992.
[9] K. Y. Lee, J. H. Cha, and K. P. Park, "Dynamic response of a floating crane in waves by considering the nonlinear effect of hydrostatic force," *Ship Technology Research*, vol. 57, no. 1, pp. 62-71, 2010.
[10] D. C. Kring, “Time domain ship motions by a three-dimensional rankine panel method,” MIT, Ph.D. Thesis, 1994.

Namkug Ku is a research engineer of Education and Research Center for Creative Offshore Plant Engineers at Seoul National University, Korea. He holds a B.S., M.S., and Ph.D. in naval architecture and ocean engineering from Seoul National University. His main area of research interests include ship and offshore plant design, multi-body dynamics, top-side process engineering of offshore plant, and so on.

Sol Ha is a research engineer of Engineering Research Institute at Seoul National University, Korea. He holds a B.S., M.S., and Ph.D. in naval architecture and ocean engineering from Seoul National University. His main area of research interests include ship and offshore plant design, methodology of modeling and simulation, risk and reliability analysis, GPU-accelerated parallel processing, fluid analysis based on lattice Boltzmann method, and so on.

Myung-Il Roh is a professor of naval architecture and ocean engineering at Seoul National University, Korea. He holds a B.S., M.S., and Ph.D. in naval architecture and ocean engineering from Seoul National University. His main area of teaching and research interests include ship and offshore plant design, simulation-based design and production, optimization, CAD, CAM, CAE, CAPP, and so on.